

Cite this article as: Gao Wei, Liu Jiangnan, Ding Zhisong, et al. Influence of Si_3N_4 Nanoparticles on Microstructure and Properties of Microarc Oxidation Coatings on TC4 Alloy[J]. Rare Metal Materials and Engineering, 2022, 51(05): 1537-1542.

ARTICLE

Influence of Si_3N_4 Nanoparticles on Microstructure and Properties of Microarc Oxidation Coatings on TC4 Alloy

Gao Wei, Liu Jiangnan, Ding Zhisong, Zhang Yong, Yao Yuhong, Yang Wei

School of Materials Science and Chemical Engineering, Xi'an Technological University, Xi'an 710021, China

Abstract: TC4 titanium alloy was treated by microarc oxidation (MAO) with adding Si_3N_4 nanoparticles into the base electrolyte. The effect of the Si_3N_4 content on the surface morphology, corrosion resistance, and wear resistance of the coatings was studied. The results show that MAO coatings with Si_3N_4 addition present the porous structure, and the coating is the thickest when the Si_3N_4 content is 1 g/L. The coating with the addition of 1 g/L Si_3N_4 after acid corrosion test for 7 d shows excellent corrosion resistance with the lowest corrosion rate of about $0.057 \text{ mg}\cdot\text{cm}^{-2}\cdot\text{d}^{-1}$. With the addition of Si_3N_4 , the antibacterial property of MAO coatings is firstly increased and then decreased, which is optimal when the Si_3N_4 addition is 1 g/L. The Si_3N_4 addition can obviously enhance the wear resistance of the coatings in the simulated seawater. When the Si_3N_4 addition is 3 and 4 g/L, the friction coefficient of MAO coatings is low and stable. In addition, MAO coating with the addition of 3 g/L Si_3N_4 shows the excellent wear resistance.

Key words: TC4 alloy; microarc oxidation; Si_3N_4 nanoparticles; microstructure; properties

Due to the low density, high specific strength, and good biocompatibility, titanium and its alloys have been widely studied and applied in biomedical, aerospace, and marine fields^[1-5]. The low surface hardness and poor tribological properties of titanium alloys lead to serious surface wear and degradation, especially in corrosive environment, which restricts the application in marine field^[6-10]. Surface treatment is a feasible way to improve the properties of titanium alloys. Microarc oxidation (MAO), namely the spark plasma electrolytic oxidation^[11-14], has been developed in recent years to improve the properties of Ti, Mg, Al, and the related alloys through arc discharge on the substrates by electric breakdown^[4,5,15]. Due to the complex physical, chemical, and electrochemical reactions during MAO process, various factors, such as the electrolyte, electrical parameters, and substrate materials, may exert an influence on the alloy properties. Additionally, the properties of MAO coatings can be improved by doping nanoparticles into electrolyte^[7,16-20].

Since Si_3N_4 has high hardness, fine lubrication, and good wear resistance, it is widely used in ceramic manufacture as the reinforcement phase^[21-23]. In order to improve the wear

resistance of titanium alloys, the composite coatings on titanium alloys via MAO with Si_3N_4 particles doped into the electrolytes were investigated^[21]. Lou et al^[24] investigated the influence of the addition of Si_3N_4 particles into the electrolyte on the microstructure, mechanical performance, and anticorrosion property of MAO coatings on AZ31 Mg alloy. It is found that the corrosion resistance of the coatings achieves the optimal state after addition of 2 g/L Si_3N_4 to the electrolyte, and the coatings have a low coefficient of friction and good adhesion strength.

In this research, in order to improve the surface properties of titanium alloys to meet the requirements of the marine environment, the effects of Si_3N_4 nanoparticles with different addition contents on the surface morphologies, corrosion resistance, wear resistance in the simulated seawater, and antibacterial property of MAO coatings were studied. Furthermore, the optimal content of Si_3N_4 nanoparticle addition in the base electrolyte was obtained.

1 Experiment

TC4 alloy plates with the diameter of 20 mm and thickness

Received date: August 27, 2021

Foundation item: National Natural Science Foundation of China (52071252); Key Research and Development Program of Shaanxi Province (2021ZDLSF03-11, 2021GY-208)

Corresponding author: Yang Wei, Ph. D., Professor, School of Materials Science and Chemical Engineering, Xi'an Technological University, Xi'an 710021, P. R. China, Tel: 0086-29-86173324, E-mail: yangwei_smx@163.com

Copyright © 2022, Northwest Institute for Nonferrous Metal Research. Published by Science Press. All rights reserved.

of 4 mm were polished with 240#, 600#, 800#, 1000#, 1500#, and 2000# sandpaper and ultrasonically cleaned with ethanol for 10 min as the substrate preparation. During the MAO process, TC4 alloy was used as the anode and the stainless steel barrel containing the electrolyte was used as the cathode. Meanwhile, the substrate was completely immersed in the electrolyte. The electrolyte was composed of $(\text{NaPO}_3)_6 + \text{Na}_2\text{WO}_4 + \text{KF} + \text{KOH} + \text{CuSO}_4 + \text{C}_6\text{H}_5\text{Na}_3\text{O}_7$. In addition, different contents of Si_3N_4 nanoparticles (1, 2, 3, and 4 g/L) with diameter of 50 nm were added into the electrolyte. The $\text{C}_{18}\text{H}_{29}\text{NaO}_3\text{S}$ (1 g/L) was also added to disperse the electrolyte. The electrolyte temperature was kept below 40 °C. MAO coatings were obtained under the constant voltage of 450 V, frequency of 750 Hz, and duty ratio of 3% for 10 min. Finally, the coated specimens were rinsed in the deionized water and dried.

The scanning electron microscope (SEM) and energy dispersive spectroscopy (EDS) were used to characterize the morphologies and element distribution of MAO coatings. The coating thickness was measured with a thickness gauge. The coated specimens were tested by the friction test with GCr15 grinding materials under the wear load of 500 g for 30 min. The friction coefficient curves of the coatings with different Si_3N_4 addition contents were obtained. The common staphylococcus aureus was used to test the antibacterial activity of MAO coatings. The cocci were inoculated in Luria-Bertani (LB) medium and activated at 37 °C for 24 h. The specimens were put into 12 plates, and then the simulated sea water was poured into the plate. The activated bacteria were added into the plate and cultured for 3 d. After that, the specimens were taken out and dried. The bacteria adhesion on the specimen surface was observed by SEM. The corrosion resistance of the coated specimens was tested in 0.5 mol/L

hydrochloric acid for 7 d, and the specimens during corrosion test were washed in alcohol, dried, and weighed every 2 d.

2 Results and Discussion

2.1 Morphologies of MAO coatings

Fig. 1 shows the surface morphologies of MAO coatings with different addition contents of Si_3N_4 particles. These five MAO coating morphologies are similar, all showing porous structures, and the diameter of “volcanic vent” is relatively uniform of 5–6 μm . During MAO process, the alloys are molten by the high voltage electric field and high current, and then enter the cold electrolyte, thereby leaving micropores on MAO coatings^[25]. Furthermore, there are a few microcracks in MAO coatings, because a large amount of heat generated by the interface between the electrolyte and the coating cannot be transmitted in time. Therefore, a large amount of thermal stress exists in the interior coating, forming the microcracks^[8].

Fig. 2 shows the thickness of MAO coatings with different contents of Si_3N_4 addition. It can be seen that the four MAO coatings with Si_3N_4 addition are thicker than the coating without Si_3N_4 addition, which is consistent with Ref.[17]. The Si_3N_4 in the electrolyte enters MAO coating in-situ by electrophoretic effect, so the coating is thicker than the coating without adding Si_3N_4 particles. Thus, due to the positive direct current pulse of MAO process, the negatively charged ions (because Si_3N_4 particles adsorb charged particles in the solution, the unequal absorption of anions and cations in the solution shows negative electricity) tend to move to the anode substrate in the electrolyte^[26]. With MAO process continuously proceeding, the number of these particles in MAO coating is increased and therefore the coating becomes thicker^[27]. In particular, when the Si_3N_4 content is 1 g/L, the thickness of related coating is the largest of 22.39 μm .

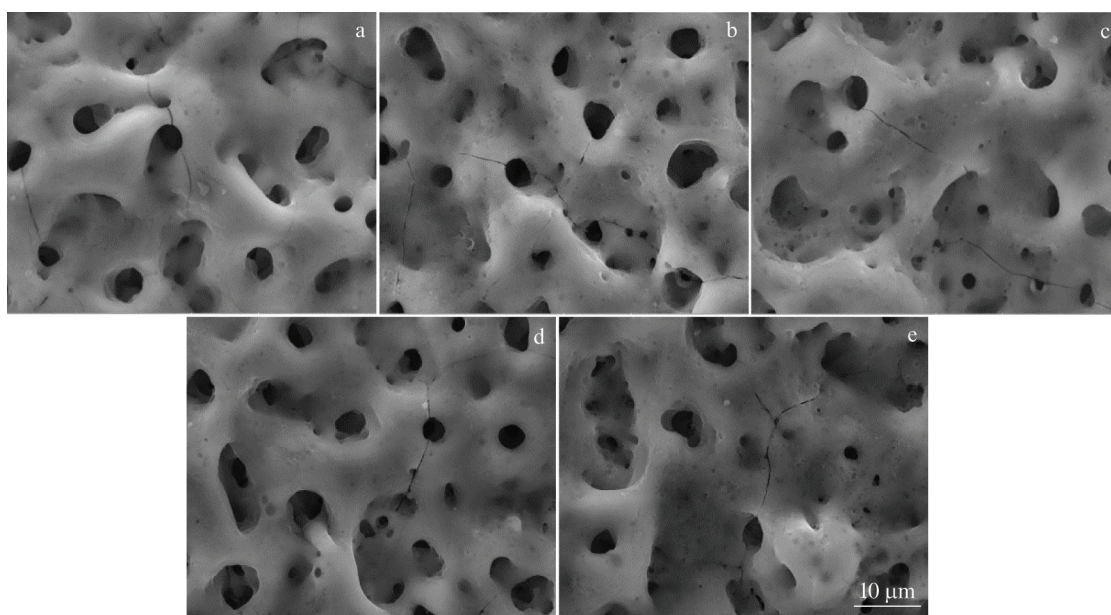


Fig.1 Surface morphologies of MAO coatings with different Si_3N_4 addition contents: (a) 0 g/L, (b) 1 g/L, (c) 2 g/L, (d) 3 g/L, and (e) 4 g/L

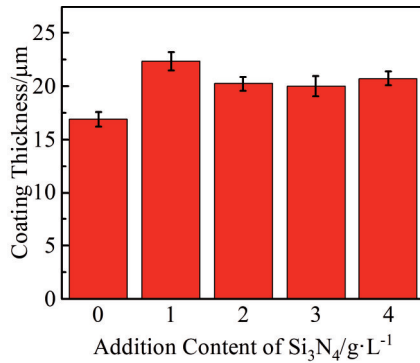


Fig.2 Thickness of MAO coatings with different Si₃N₄ addition contents

The binding states of coated specimens were investigated by X-ray photoelectron spectroscopy (XPS). Fig. 3a shows XPS spectra of ceramic coatings with Si₃N₄ addition. It can be seen that Ti, Al, Si, O, and C elements exist in TC4 alloy substrate. The C 1s signal peak from the external carbonaceous organism is used as the calibration. Fig. 3b~3d show XPS spectra of Ti 2p, Al 2p, and Si 2p of MAO coating with Si₃N₄ addition, respectively. Fig. 3b indicates that the titanium exists as Ti⁴⁺. The Ti 2p spectra exhibit two peaks at 458.7 (Ti 2p_{3/2}) and 464.7 (Ti 2p_{1/2}) eV, indicating the TiO₂ existence^[28]. The Al 2p spectra of coatings show only one peak at the binding energy of 74.6 eV, indicating the existence of the Al₂O₃ in the coating^[29]. Furthermore, it is found that TiO₂ and Al₂O₃ are formed by the combination of Ti and Al from the substrate and O from the external environment. The peak at

101.2 eV of Si 2p spectra corresponds to the characteristic peak of Si₃N₄, suggesting that the Si₃N₄ nanoparticles enter the MAO coating.

2.2 Corrosion resistance of MAO coatings

The corrosion rates of MAO coatings with different Si₃N₄ addition contents immersed in hydrochloric acid for 7 d are shown in Fig. 4. It is found that the corrosion rates of the obtained coatings are firstly increased and then decreased. At the initial stage of corrosion, due to the existence of micropores and cracks on MAO coating surface, Cl⁻ in hydrochloric acid directly contacts with the substrate through the coating, forming many tiny corrosion galvanic cells, which results in higher corrosion rates. After that, the corrosion rate is reduced because the corrosion ion further corrodes the matrix through micropores and cracks. After corrosion for 7 d, the MAO-coated specimen with 1 g/L Si₃N₄ shows the lowest corrosion rate of 0.057 mg·cm⁻²·d⁻¹, because this MAO coating is the thickest, and the inhibition effect on corrosion ion is more obvious. The final corrosion rate of the four coatings with Si₃N₄ addition is all lower than that without Si₃N₄ addition. Although the ceramic coatings with Si₃N₄ addition are coarser, the chemical stability of Si₃N₄ in the ceramic coating plays an important role in the corrosion resistance of the coatings.

Fig. 5 shows the corrosion morphologies of MAO-coated specimens in hydrochloric acid for 7 d. With increasing the content of Si₃N₄ particles, the corrosion of the coated specimens becomes serious, and the diameter of micropores and the number of microcracks on the coatings are increased gradually. When the Si₃N₄ content is 1 g/L, the coating is

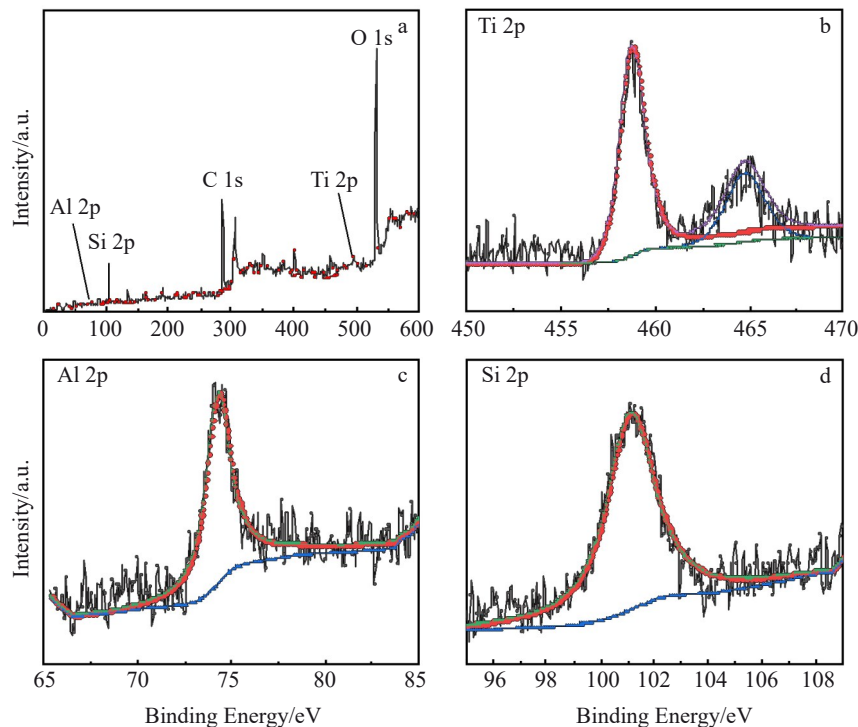


Fig.3 XPS spectra of MAO-coated specimens with Si₃N₄ addition of 4 g/L: (a) total; (b) Ti 2p; (c) Al 2p; (d) Si 2p

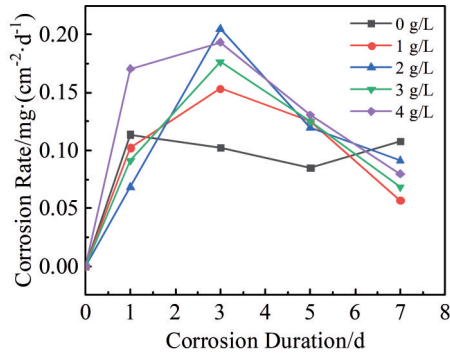


Fig.4 Corrosion rates of different MAO-coated specimens in hydrochloric acid

intact without obvious corrosion trace. When the Si_3N_4 content is 4 g/L, the coating is rougher than others, although the Si_3N_4 nanoparticles are inert particles. The corrosion of the coating is serious, because Cl^- in the corrosion solution can enter the micropores of the coating, which accelerates the further corrosion. Meanwhile, the microcracks of the coating are increased slightly, compared with those before corrosion. Although the corrosion products gradually accumulate in the micropores of the coating, it can avoid the contact between the corrosion ions and the coating, inhibiting the corrosion process. Finally, with the corrosion process proceeding, the accumulation of a large number of corrosion products leads to the increase in microcracks of coating, even resulting in the coating falling off from the TC4 substrates^[7,18].

2.3 Antibacterial properties of MAO coatings

SEM morphologies of staphylococcus aureus adhesion on MAO coatings with different contents of Si_3N_4 addition are

shown in Fig.6. It is obvious that many bacteria are attached to MAO coating without Si_3N_4 addition, so its antibacterial performance is poor. When the Si_3N_4 addition is 1 g/L, the antibacterial property of MAO coating is the optimal with the least bacteria attached to the coating surface. The antibacterial performance of MAO coatings is determined by the lubricity characteristic of Si_3N_4 particles and the roughness of coating surface. As shown in Fig.6c, when the Si_3N_4 addition is 2 g/L, more bacteria are attached to MAO coating, compared with those with the addition of 1 g/L Si_3N_4 . Besides, MAO coating surface with the addition of 1 g/L Si_3N_4 is rougher than that of 2 g/L Si_3N_4 . Therefore, the antibacterial performance of MAO coating surface of 2 g/L Si_3N_4 is reduced. It can be seen from Fig. 6d and 6e that the bacteria are slightly increased, suggesting even more inferior antibacterial performance. This can be attributed to the micro-bumps formed by Si_3N_4 particles on the MAO coating, which are easy to be attached by the bacteria.

2.4 Wear resistance of MAO coatings

As shown in Fig.7, the friction coefficient of MAO coatings with different contents of Si_3N_4 is firstly increased and then decreased in the simulated seawater, because in the early stage of wear, the coatings are mainly damaged by the surface protrusion. With further applying the shear stress, the wear debris generated in the early stage of wear test enters the micropores of the coatings, therefore reducing the friction coefficient. Then, the micropores of the coating are filled and the excess wear debris occurs, resulting in the slightly increasing friction coefficient. In addition, it can be seen from Fig. 7 that the Si_3N_4 addition in the four MAO-coated specimens has a positive influence on the friction coefficient, i. e., the friction coefficient of MAO-coated specimen with

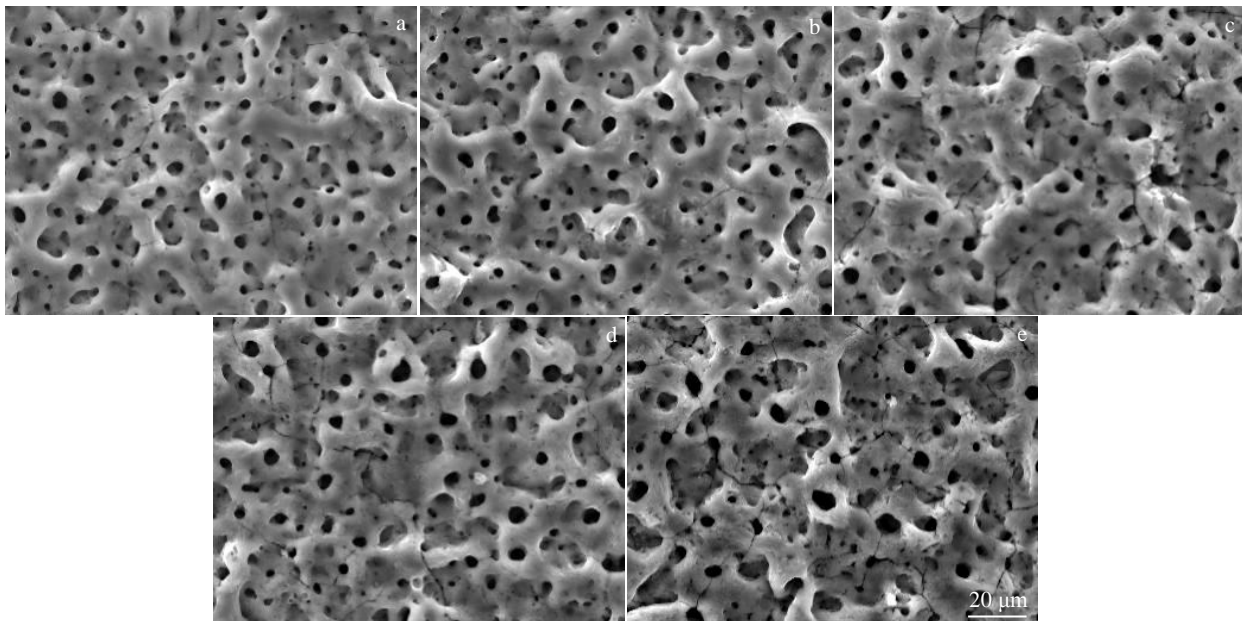


Fig.5 Corrosion morphologies of MAO-coated specimens with different Si_3N_4 addition contents in hydrochloric acid for 7 d: (a) 0 g/L, (b) 1 g/L, (c) 2 g/L, (d) 3 g/L, and (e) 4 g/L

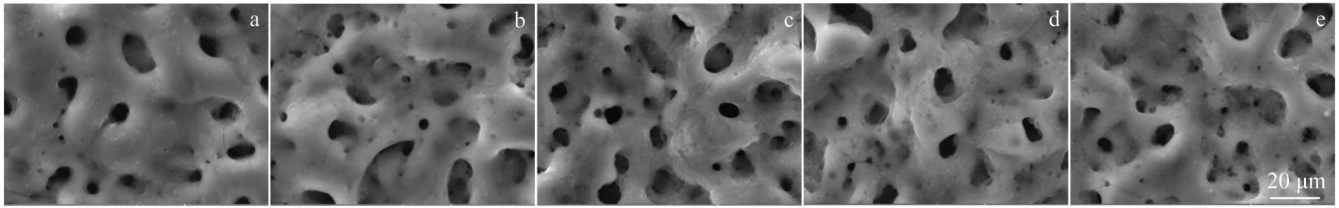


Fig.6 SEM morphologies of bacterial adhesion on MAO coatings with different Si_3N_4 addition contents: (a) 0 g/L, (b) 1 g/L, (c) 2 g/L, (d) 3 g/L, and (e) 4 g/L

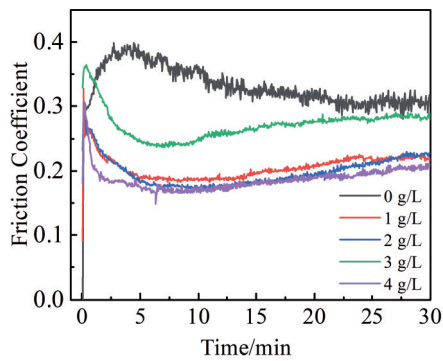


Fig.7 Friction coefficients of different MAO-coated specimens in simulated seawater

Si_3N_4 addition is small and stable, compared with that of the MAO coating without Si_3N_4 addition. When the addition content of Si_3N_4 is 3 and 4 g/L, the friction coefficients of the obtained coatings are relatively small (below 0.2) in the whole wear process. So the Si_3N_4 addition can improve the wear resistance of the coating and significantly reduce the friction

coefficient. Although the Si_3N_4 addition in MAO coating results in the generation of micro-bulge (green circle in Fig. 8a), the friction coefficient of the coating is obviously decreased due to excellent lubrication characteristic of Si_3N_4 .

SEM images and Fe element distributions of the wear scars of MAO coatings with different contents of Si_3N_4 addition in the simulated seawater are shown in Fig.8. It can be seen from Fig. 8a and 8b that a lot of wear products are formed on the MAO coatings with and without Si_3N_4 addition, and the wear failure mode is abrasive wear due to the uneven coating surface. When the Si_3N_4 addition is 2 and 4 g/L, MAO coatings are peeled off locally from the substrates, and corrosion pits (red circles in Fig. 8c and 8e) are formed by the corrosive simulated seawater, which reduces the protective effect and results in the failure of coatings. MAO coating with the addition of 3 g/L Si_3N_4 is not obviously damaged and the adhesion of wear products on this MAO coating is less. The friction coefficient of this coating is also small and stable during the wear process, so MAO coating with the addition of 3 g/L Si_3N_4 has the optimal wear resistance in the simulated seawater. It is also found that the Fe element from GCr15 grinding materials moves to the surface of all MAO coatings

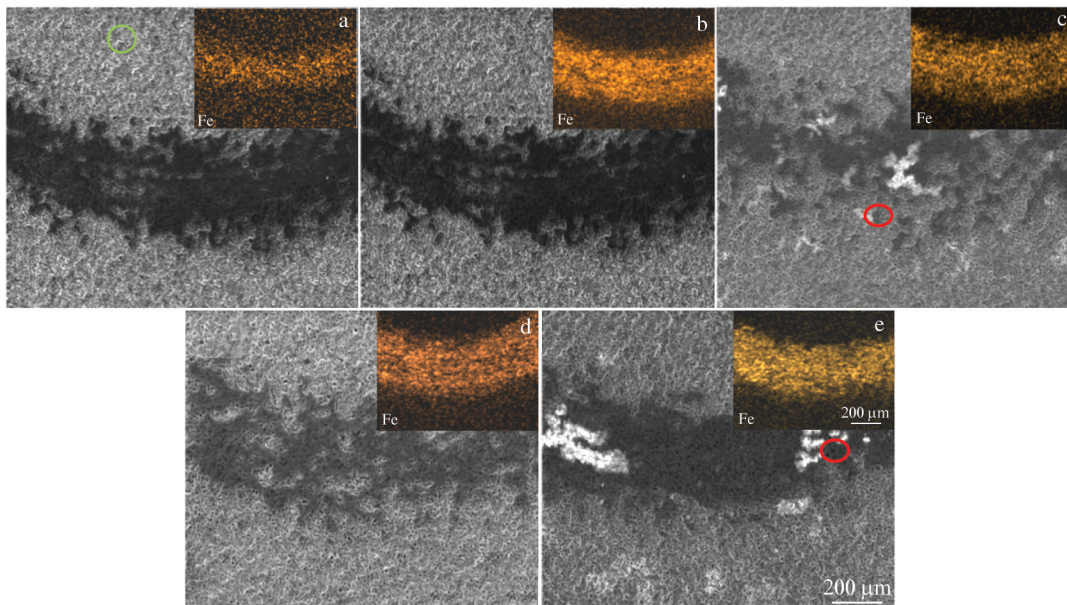


Fig.8 Wear morphologies and Fe element distributions of MAO-coated specimens with different Si_3N_4 addition contents in simulated seawater: (a) 0 g/L, (b) 1 g/L, (c) 2 g/L, (d) 3 g/L, and (e) 4 g/L

and the distribution of Fe element in the wear scars is uniform. In general, the appropriate addition of Si_3N_4 can balance the lubrication properties and the generation of abrasive particles, thus leading to the excellent wear resistance of MAO-coated specimens.

3 Conclusions

1) The microarc oxidation (MAO) coatings with Si_3N_4 addition have the porous structure with the diameter of 5~6 μm . The thickness of MAO coatings with Si_3N_4 addition is increased, compared with that without Si_3N_4 addition. MAO coating has the maximum thickness of 22.39 μm when the Si_3N_4 addition is 1 g/L.

2) The corrosion rate of MAO coating with the addition of 1 g/L Si_3N_4 is the slowest of about $0.057 \text{ mg}\cdot\text{cm}^{-2}\cdot\text{d}^{-1}$.

3) MAO coatings with Si_3N_4 addition show excellent antibacterial property. As the Si_3N_4 addition content is 1 g/L, the least bacteria are attached to the coating surface.

4) The Si_3N_4 addition in MAO coatings has a positive influence on the friction coefficient, i. e., the friction coefficient of MAO coating without Si_3N_4 addition is small and stable. In particular, MAO coating with the addition of 3 g/L Si_3N_4 has the optimal wear resistance in the simulated seawater.

References

- 1 Kurup A, Dhattrak P, Khasnis N. *Materials Today: Proceedings* [J], 2021, 39(Part 1): 84
- 2 Liao S C, Chang C T, Chen C Y et al. *Surface and Coatings Technology*[J], 2020, 394: 125 812
- 3 Quintero D, Galvis O, Calderón J A et al. *Surface and Coatings Technology*[J], 2015, 283: 210
- 4 Wang T, Wang L, Lu Q et al. *J Prosthet Dent*[J], 2019, 121: 156
- 5 Ouyang J H, Wang Y H, Liu Z G et al. *Wear*[J], 2015, 330-331: 239
- 6 Madhavi Y, Narasaiah N, Jyothirmayi A et al. *Surface and Coatings Technology*[J], 2021, 414: 127 102
- 7 Yang W, Xu D P, Wang J L et al. *Corrosion Science*[J], 2018, 136: 174
- 8 Lin J Z, Chen W D, Tang Q Q et al. *Surfaces and Interfaces*[J], 2021, 22: 100 805
- 9 Lv X Y, Zou G P, Ling K et al. *Surface and Coatings Technology* [J], 2021, 406: 126 630
- 10 Fazel M, Shamanian M, Salimijazi H R. *Biotribology*[J], 2020, 23: 100 131
- 11 Tchufistov O E, Tchufistov E A. *Materials Today: Proceedings* [J], 2019, 19: 2013
- 12 Lan N, Yang W, Gao W et al. *Diamond and Related Materials* [J], 2021, 117: 108 483
- 13 Songur F, Dikici B, Niinomi M et al. *Surface and Coatings Technology*[J], 2019, 374: 345
- 14 Huang Q, Wu Z Z, Wu H et al. *Surface and Coatings Technology* [J], 2019, 374: 1015
- 15 Yang W, Wang J L, Xu D P et al. *Surface and Coatings Technology*[J], 2015, 283: 281
- 16 Molaei M, Nouri M, Babaei K et al. *Surfaces and Interfaces*[J], 2021, 22: 100 888
- 17 Muhaffel F, Kaba M, Cempura G et al. *Surface and Coatings Technology*[J], 2019, 377: 124 900
- 18 Zheng Z, Zhao M C, Tan L et al. *Surface and Coatings Technology*[J], 2020, 386: 125 456
- 19 Daroonparvar M, Yajid M A M, Yusof N M et al. *Journal of Alloys and Compounds*[J], 2016, 688: 841
- 20 Ge Y L, Wang Y M, Zhang Y F et al. *Surface and Coatings Technology*[J], 2017, 309: 880
- 21 Dhakal D R, Kshetri Y K, Gyawali G et al. *Applied Surface Science*[J], 2021, 541: 148 403
- 22 Li L C, Ding M, Lin B et al. *Tribology International*[J], 2021, 159: 169 968
- 23 Llorente J, Ramírez C, Belmonte M. *Journal of the European Ceramic Society*[J], 2020, 40: 5298
- 24 Lou B S, Lin Y Y, Tseng C M et al. *Surface and Coatings Technology*[J], 2017, 332: 358
- 25 Li Y K, Chen M F, Li W et al. *Surface and Coatings Technology* [J], 2019, 358: 637
- 26 Lu X P, Blawert C, Huang Y et al. *Electrochimica Acta*[J], 2016, 187: 20
- 27 Lu X P, Mohedano M, Blawert C et al. *Surface and Coatings Technology*[J], 2016, 307(C): 1165
- 28 Frauchiger V M, Schlottig F, Gasser B et al. *Biomaterials*[J], 2004, 25: 593
- 29 Cheng Y L, Xue Z G, Wang Q et al. *Electrochimica Acta*[J], 2013, 107: 358

纳米 Si_3N_4 对TC4钛合金微弧氧化层微观结构和性能的影响

高 巍, 刘江南, 丁智松, 张 勇, 要玉宏, 杨 巍

(西安工业大学 材料与化工学院, 陕西 西安 710021)

摘 要: 在基电解液中加入氮化硅纳米颗粒, 对TC4钛合金进行微弧氧化(MAO)处理, 研究了 Si_3N_4 浓度对微弧氧化层表面形貌、耐腐蚀性和耐磨性的影响。添加 Si_3N_4 的MAO层呈现多孔结构, 当 Si_3N_4 浓度为1 g/L时, 涂层厚度最大, 且经过7 d的酸腐蚀试验, 该涂层的耐蚀性良好, 腐蚀速率最低, 约为 $0.057 \text{ mg}\cdot\text{cm}^{-2}\cdot\text{d}^{-1}$ 。随着 Si_3N_4 的加入, MAO涂层的抗菌性能先升高后降低。当 Si_3N_4 的添加量为1 g/L时, 该MAO层的抗菌性能最好。 Si_3N_4 的加入能明显提高涂层在模拟海水中的耐磨性。当 Si_3N_4 的添加量为3和4 g/L时, 所得涂层的摩擦系数低且稳定, 且添加3 g/L Si_3N_4 制备来的MAO涂层表现出优异的耐磨性。

关键词: TC4钛合金; 微弧氧化; Si_3N_4 纳米颗粒; 微观结构; 性能

作者简介: 高 巍, 男, 1977年生, 博士, 副教授, 西安工业大学材料与化工学院, 陕西 西安 710021, 电话: 029-86173324, E-mail: yangwei_smx@163.com